

Galaxy morphology prediction using capsule networks

Reza Katebi^{1*}, Yadi Zhou², Ryan Chornock¹ and Razvan Bunescu³

¹*Astrophysical Institute, Department of Physics and Astronomy, Ohio University, Athens, OH 45701, USA*

²*Department of Chemistry and Biochemistry, Ohio University, Athens, OH 45701, USA*

³*School of Electrical Engineering and Computer Science, Ohio University, Athens, OH 45701, USA*

Accepted XXX. Received YYY; in original form ZZZ

ABSTRACT

Understanding morphological types of galaxies is a key parameter for studying their formation and evolution. Neural networks that have been used previously for galaxy morphology classification have some disadvantages, such as not being invariant under rotation. In this work, we studied the performance of Capsule Network, a recently introduced neural network architecture that is rotationally invariant and spatially aware, on the task of galaxy morphology classification. We designed two evaluation scenarios based on the answers from the question tree in the Galaxy Zoo project. In the first scenario, we used Capsule Network for regression and predicted probabilities for all of the questions. In the second scenario, we chose the answer to the first morphology question that had the highest user agreement as the class of the object and trained a Capsule Network classifier, where we also reconstructed galaxy images. We achieved promising results in both of these scenarios. Automated approaches such as the one introduced here will greatly decrease the workload of astronomers and will play a critical role in the upcoming large sky surveys.

Key words: methods: data analysis – galaxy: general – techniques: image processing – catalogs

1 INTRODUCTION

Morphological classifications have been used by astronomers to classify galaxies based on their visual aspects such as size, colour and shape. Studying morphological classifications is crucial to understand the evolution of galaxies and their properties such as age, formation and interaction with other galaxies. All-sky surveys are the key solutions to probe galaxy formation and evolution.

In order to conduct these studies, observation of a large number of galaxies and determination of their morphological classification is crucial. Large sky surveys such as the Sloan Digital Sky Survey (SDSS) (e.g., Blanton et al. 2017) provided a large amount of data for the objects in our universe including galaxies. The morphological classification of galaxies has been traditionally done by experts, which is both inefficient and impractical for the large datasets available from current sky surveys and even larger upcoming ones such as the Large Synoptic Survey Telescope (LSST) (Ivezic et al. 2008). The Galaxy Zoo project (Lintott et al. 2008) started with the hope of partially solving this problem by a crowdsourcing method. The project was very successful and ~ 900,000 galaxies were classified by online participants in a time span of months. Since then, other iterations

of the Galaxy Zoo project have annotated other datasets with more complex classification schemes (e.g., Willett et al. 2016). However, even this approach is not feasible for the available and upcoming large datasets.

The amount of data is increasing as modern telescopes continue to take data, and projects like LSST will significantly increase the number of galaxies observed. Therefore, classifying these galaxies by crowdsourcing and visual inspection is next to impossible and developing an automated classification tool is necessary. Recently, improvement in computer vision techniques primarily through deep neural networks (e.g., Krizhevsky et al. 2012) and available computing power through GPUs have made this automated approach more promising.

In an attempt to find an automated classification approach, an international competition was launched by Galaxy Zoo on Kaggle¹ using the images from the Galaxy Zoo 2 project (Willett et al. 2013) and the winning team provided a convolutional neural network (CNN) that exploits both translational and rotational symmetry in the images. This method can produce near perfect accuracy of > 99% for the images with a high agreement among the Galaxy Zoo participants (Dieleman et al. 2015). However, in order

* E-mail: rk726014@ohio.edu

¹ <https://www.kaggle.com/c/galaxy-zoo-the-galaxy-challenge>

to extract the viewpoint, Dieleman et al. (2015) flipped, rotated and cropped images to extract 16 viewpoints for each image. Next, they trained a neural network with 16 convolutional neural subnetworks for each of the extracted viewpoints that are all connected to two fully connected layers. Each of these subnetworks learns the same features in a particular viewpoint that are useful for the classification task (Dieleman et al. 2015). However, the problem with this approach is that it cannot cover all of the possible rotations, orientations and their combinations; therefore, it still heavily depends on different training setups. Another problem is that this method is computationally very expensive because it relies on training multiple subnetworks. Moreover, it has been known that CNNs lose valuable information such as spatial hierarchies between features in the image. They also lack rotational invariance that causes CNNs to incorrectly assign labels to objects as long as a set of features is present during the test time disregarding the spatial relationship of these features to each other (Sabour et al. 2017).

Recently, Sabour et al. (2017) introduced a new type of network structure called Capsule Network (CapsNet) to address these issues in CNNs. This new structure contains capsules that are a nested set of layers. In contrast to traditional CNNs, this network is spatially aware and rotationally and translationally invariant with the use of dynamic routing and reconstruction as regularization. Sabour et al. (2017) achieved state of the art result of 0.25% test error on the Modified National Institute of Standards and Technology (MNIST) dataset of handwritten digits with shifting the images only by two pixels without applying any other data augmentation methods (e.g., rotation, flipping, scaling, etc.). In this work, we are proposing the use of CapsNet for the task of galaxy morphology prediction as a better alternative for CNNs.

2 GALAXY ZOO 2

The Galaxy Zoo is an online project where participants described galaxy morphology classification by answering a series of questions on the coloured images of the galaxies. In this work, we used data from the Galaxy Zoo 2 project where the participants answered 11 questions with 37 answers in total (Willett et al. 2013). These questions were designed in a hierarchical manner where the next question was chosen based on the answer of the participant to the previous question. Each individual answered a subset of questions based on the way the decision tree was designed. The answers provided by users for one image transformed to a set of weighted vote fractions. These results have been used to study structure, formation and evolution of the galaxies (e.g., Skibba et al. 2009). Also, the accuracy of the results from the Galaxy Zoo projects was confirmed by comparing them with smaller samples classified by experts and automated pipelines (Bamford et al. 2009; Willett et al. 2013). Here, we used the dataset provided by Galaxy Zoo 2 for an international contest. The galaxies were selected with a variety of colours, sizes, and morphological classes. The goal of the project was to find an algorithm that could be applied to many different types of galaxies in the upcoming surveys. The total number of objects was limited by the depth of imaging in SDSS and the morphological categories

that were over-represented as a function of the colour. This approach ensured that the colour does not play a role in the morphological classification and the models are purely based on the structures of the galaxies observed in the images. We only used the training set of the provided dataset because we did not have access to the labels of the validation dataset. The training set consisted of 61,578 JPEG coloured images of the galaxies with the size of 424×424 pixels. The morphological data was in the form of cumulative probabilities that gave higher weights to the questions that were asked higher in the question tree and determined a more fundamental morphological structure.

The goal of the contest was to predict probabilities for each of the 37 answers in the question tree; therefore, the task was a regression as opposed to classification. However, in this work we also reconstructed galaxy images based on the answers to question 1. This classification scheme is discussed in Section 4 in more detail.

3 RELATED WORK

Machine learning techniques such as neural networks have been used in astronomy research in the past few decades (e.g., photometric redshift estimation; Collister & Lahav 2004; Firth et al. 2003). Galaxy morphology classification is traditionally done by manually extracting a number of features that are known to discriminate different classes. Examples of these features are: surface brightness, ellipticity, concentration, radii, and log-likelihood values measured from different types of radial profiles (e.g., Storrie-Lombardi et al. 1992).

Storrie-Lombardi et al. (1992) used feed forward neural networks and 13 extracted parameters as input for training a classifier. Subsequent works used other machine learning methods such as kernel support vector machines (SVMs) (Tasca et al. 2009) and principal component analysis (PCA) (Naim et al. 1995; Lahav et al. 1995; De La Calleja & Fuentes 2004) to extract features from the images. Next, they trained feed-forward neural networks using these features. These methods still heavily rely on feature extraction. In another approach, researchers used general purpose image features rather than galaxy-specific ones to perform galaxy morphology classification combined with nearest-neighbor classifiers (e.g., Kuminski et al. 2014).

Recently, Dieleman et al. (2015) used CNNs for this task. Their approach is different from the ones introduced before in two ways. First, the morphological classification scheme provided by Galaxy Zoo 2 was a much more fine-grained task compared to the past work (mentioned above) where the task was classifying galaxies into a limited number of morphological classes (except Kuminski et al. 2014). Second, they did not use any prior handcrafted features or features that were extracted using machine learning algorithms such as PCA and SVM, which typically need many hours to develop. Instead, their proposed deep neural network learns hierarchies of features that allow the network to detect more abstract and complex features in the images.

One important aspect of their approach is that their method exploits rotational and translational symmetry in the images. To do that, they constructed 16 different viewpoints for each image by rotating, cropping, and flipping

the image. Next, they have used one CNN with 4 convolutional plus pooling layers for each of these viewpoints and connected all 16 CNNs to two fully connected layers that were regularized using dropout method (Hinton et al. 2012). However, their method cannot cover all of the possible rotations, orientations, and their combinations; therefore, it still heavily depends on pre-training data manipulations. Moreover, there are disadvantages for using CNNs; specifically, they are known to lose important information about the spatial hierarchies between features in the image during the pooling process (usually max pooling) or, in other words, they are not spatially aware (Sabour et al. 2017). In our approach, we used CapsNet, which was proposed to solve the problems of CNNs that were discussed above. CapsNet is rotationally and transitionally invariant because it uses a unique type of algorithm called “routing by agreement” and applies reconstruction as regularization. We will discuss the structure of CapsNet in the Section 4.3 in more details.

4 APPROACH

In this section, we discuss our approach for galaxy morphology classification that is quite different from other ones proposed earlier. First, we discuss our experimental setup. Next, we talk about the preprocessing that we did in order to prepare the data for training. Last, we discuss the network structure, training process and our implementation.

4.1 Experimental Setup

The dataset that we used contains 65,578 images with associated portabilities of 37 answers of the questions asked during Galaxy Zoo 2 project. The task on the competition was to predict the probabilities for each of these 37 answers and calculate a root-mean-square-error (RMSE). We took two approaches here. In the first approach, we calculated RMSE, which was the goal of competition. In the second scenario, we took only the answers to the first question as the ground truth and chose objects where annotators had more than 0.8 agreement on choosing one answer where the participants chose among the first two answers. Therefore, we assigned two classes to the training examples based on the answer with the highest probability. In both evaluation scenarios, we divided the dataset to 80% training and 20% testing subsets.

4.2 Data Preprocessing

We first cropped the images to reduce the dimensions of the input to the network. The majority of the objects were in the center of the images that fit in a square smaller than the size of the image; therefore, we cropped images from 424×424 pixels to 216×216 pixels and then down-sampled them 3 times to 72×72 pixels. We shifted images 2 pixels in each dimension with zero padding. We did not do any other data preprocessing and augmentation because CapsNet performs well with small datasets (Sabour et al. 2017). We did not convert coloured images to grey scale because we observed that the accuracy is higher when using the coloured version and the reason behind it is that there is colour difference

between the different parts of the galaxy such as bulge and the disk components.

4.3 Capsule Network

Capsules in CapsNet (Sabour et al. 2017) are groups of neurons that output vectors that represent different poses of the input. One of the disadvantages of the CNNs as mentioned before comes from pooling layers. In order to overcome this, CapsNet replaces pooling layers with an algorithm called “routing by agreement”. In this algorithm, the lower layer capsules or Primary capsules predict the output of the next layer capsules or parent capsules. The routing weights get stronger if these predictions have a strong agreement with the actual outputs of the parent capsules and weaker if they disagree during the routing iterations. Taking i as the activation function for the capsule i in the layer $l+1$, the predicted output $\hat{u}_{j|i}$ of the capsules in the layer $l+1$ is represented by,

$$\hat{u}_{j|i} = W_{ij}u_i \quad (1)$$

where W_{ij} is learned by the network during the backward propagation. Next, the coupling coefficients of the primary and parent capsules (c_{ij}) are calculated by applying a *Soft-max* function on the initial logits b_{ij} that are set to zero at the initial stage of the routing by agreement process,

$$c_{ij} = \frac{\exp(b_{ij})}{\sum_k \exp(b_{ik})} \quad (2)$$

where k is the number of capsules in the next layer. After that, the input layer of the parent capsules j in layer $l+1$ is calculated as follows:

$$s_j = \sum_i c_{ij}\hat{u}_{j|i} \quad (3)$$

Then, a non-linear squashing function represented in eq. 4 is applied on the output vectors to keep their length between 0 and 1 because the length of these vectors represent the probability of the presence of the object in the image,

$$v_j = \frac{\|s_j\|^2}{1 + \|s_j\|^2} \frac{s_j}{\|s_j\|} \quad (4)$$

Next, the log probabilities are updated by the actual outputs of the v_j capsules j in layer $l+1$ and the predicted outputs $\hat{u}_{j|i}$ as following,

$$b_{ij} \leftarrow b_{ij} + v_j \cdot \hat{u}_{j|i} \quad (5)$$

Each of the capsules k in the last layer is associated with a loss function l_k that has the following from,

$$l_k = T_k \max(0, m^+ - \|v_k\|)^2 + \lambda(1 - T_k) \max(0, \|v_k\| - m^-)^2 \quad (6)$$

where T_k is one when class k is present and zero otherwise. In this work, we chose $\lambda = 0.5$, $m^+ = 0.9$ and $m^- = 0.1$ for consistency with previous work (Sabour et al. 2017).

In the case of regression, we used mean-square error (MSE) between the predictions and true crowd-sourced probabilities as the loss function that is as following,

$$MSE(p'_k, p_k) = \sum_{k=1}^{37} (p'_k - p_k)^2 \quad (7)$$

where p_k is the answer probabilities associated with an image and p'_k are probabilities predicted by the network.

4.4 Network Architecture

4.4.1 Baseline Network

For the classification schemes, we used a standard CNN model with the following structure:

- 72×72 downsampled images of the galaxies as input.
- A convolution layer with 512 filters with a receptive field of 9×9 and a stride of 1.
- Max pooling with a receptive field of 2×2 and a stride of 2.
- Rectified Linear Function (ReLU) (Glorot et al. 2011; Nair & Hinton 2010) as activation function
- A convolution layer with 256 filters with a receptive field of 5×5 and a stride of 1.
- Max pooling with a receptive field of 2×2 and a stride of 2.
- ReLU as activation function
- A fully connected layer with 1024 neurons with ReLU as their activation function followed by the dropout rate of 0.5.
- A fully connected layer with 1024 neurons with ReLU as their activation function followed by the dropout rate of 0.5.
- A fully connected layer with Log-Softmax as their activation function where the number of neurons is assigned based on the number of classes in the classification scheme.

For the baseline network we used negative log-likelihood as the loss function for the classification scheme and we removed the the last fully connected layer, dropout and the Log-Softmax layer when calculating RMSE in the regression scheme.

4.4.2 Capsule Network

Our network structure was based on the original CapsNet introduced by Sabour et al. (2017) with some minor changes because of the size of the input images that is shown in Figure 1. The structure of the network was as following:

- Inputs: 72×72 downsampled images of the galaxies.
- Layer 1: a convolutional layer with 256 filters with a receptive field of 9×9 and a stride of 1 with no zero padding that lead to the 256 feature maps with the size of 64×64 .
- Layer 2: second convolutional layer with 256 filters with a receptive field of 9×9 and a stride of 2 applied and then reshaped to 32 primary capsules with 8 dimensions where each dimension is a feature map with the size of 28×28 .
- Last layer: 2 or 37 capsules based on the training scheme studied in this work where each of them represented one class.
- Decoder: the decoder part of the network was composed of three fully connected layers with 512, 1024 and 15,552 neurons respectively where the neurons in the first two had ReLU as their activation function and the neurons of the last layer had a Sigmoid activation function. The number of neurons in the last layer were equal to the number of pixels in the input image. In fact, the reconstruction loss is the squared difference between the reconstructed image and the input image and it was scaled to 0.0005, so it would not dominate during the training process.

The decoder part of the network forces the capsules to

Model	Training	Testing
Baseline	0.109	0.113
CapsNet	0.081	0.103

Table 1. Computed RMSE between the predictions and true crowd-sourced probabilities; A relative error reduction of 8.8% was achieved.

learn features during the training that are useful for the reconstruction of the image; therefore, it acts like a regularization for the network and controls the overfitting. For the regression task, we removed the decoder part of network and computed RMSE as discussed in Section 4.3.

4.5 Implementation and Resources

We implemented our model ² in Python using the Pytorch library based on the code provided in gram ai (2018) that enabled us to use GPU acceleration. Moreover, the Pytorch library carried out the differentiations with the *autograd* method. We used one NVIDIA Tesla P100 GPU unit along with 4 CPUs on the Owen cluster at the Ohio Supercomputer Center (OSC) with 16Gb of memory (Center 1987). For training our networks, we used an Adam optimizer.

5 RESULTS

5.1 Regression

In this section, we removed the decoder part of the CapsNet and computed the RMSE between the predictions and true crowd-sourced probabilities as explained in Section 4.3. We also removed the last fully connected layer, dropouts and Log-Softmax layer in the baseline model. We ran both models for 30 epochs. The baseline took 6 hours while CapsNet took 30 hours of real-time computing. One reason behind this was that our pilot study was only allocated one GPU on the cluster and we had to choose a batch size of 5 because of limited memory. We should note that in terms of the number of parameters, the baseline model has 208,961,829 while CapsNet has 124,209,845 in this training scheme. We reported the computed RMSEs in Table 1. We also show RMSE vs number of epochs in Figure 2 for both training and testing. As we can see in the results, CapsNet outperformed our baseline model.

5.2 Classification Based on Answers to Question 1 and Reconstruction of Galaxies

In this setup we only chose question one from the question tree, because this question is the most fundamental. Specifically, the question asked “Is the galaxy simply smooth and rounded, with no sign of a disk?”. There are three answers to this question that determined whether the object is round and smooth (elliptical galaxies), object with disks (spiral galaxies), or an artifact or a star. We first calculated the

² <https://github.com/RezaKatebi/Galaxy-Morphology-CapsNet>

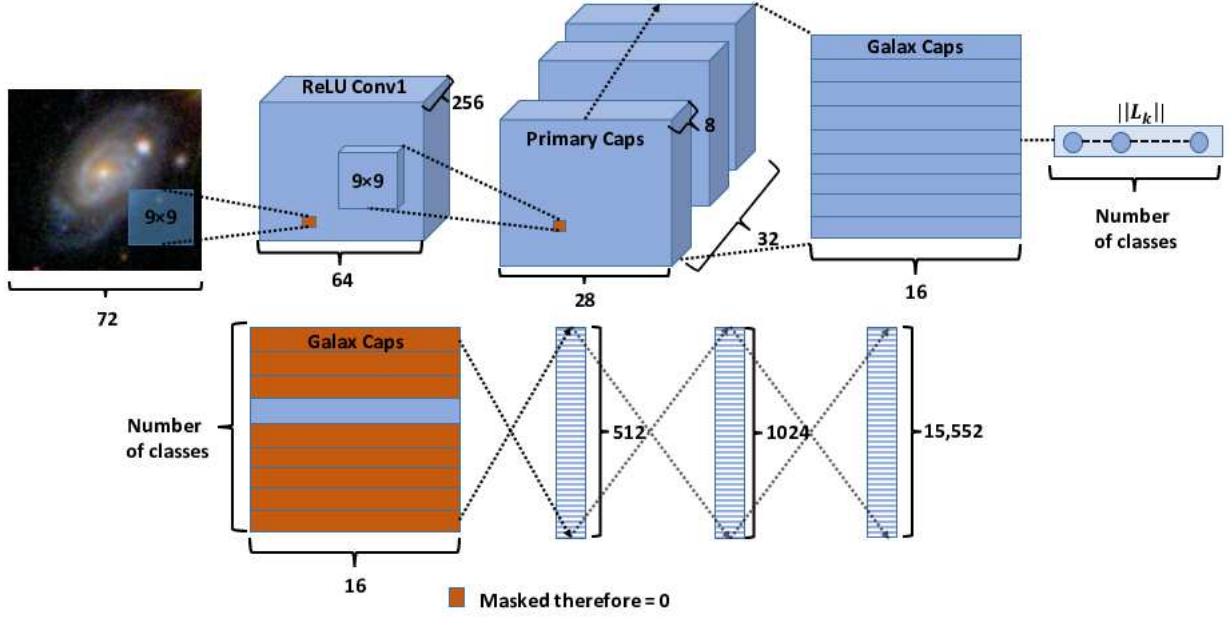
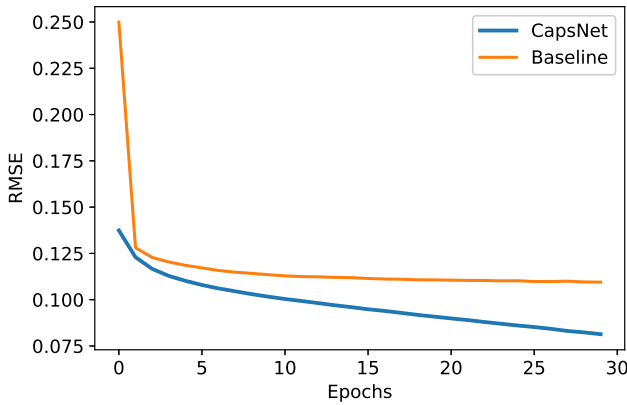
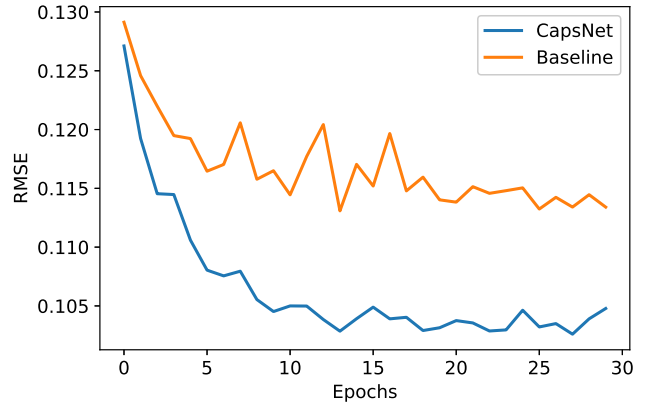


Figure 1. The architecture of the model used in this work. *Top:* represents architecture of the capsule layers where the GalaxCap layer has 2 or 37 capsules based on the different setups discussed in Section 4.4. *Bottom:* represents the structure of the decoder that acts as regularization during the training



(a) Training



(b) Testing

Figure 2. Training and testing RMSE vs number of epochs for classification based on the answers to question one.

measure of agreement using equation 7 in Dieleman et al. (2015) that reads,

$$a(p) = 1 - \frac{H(p)}{\log(n)} \quad (8)$$

where $H(p) = -\sum_{i=1}^n p(x_i) \log(p(x_i))$ is the entropy of the discrete probability distribution $p(x_i)$ over n options. The value of $a(p)$ is between 0 and 1 where 0 stands for minimal agreement and 1 stands for maximal agreement. Next, we chose the images where the measure of agreement of participants was $a(p) > 0.8$ where participants only chose between the first two answers (1.1 and 1.2; see Figure 1 and Table 2 in

Willett et al. (2013)). For this task, we picked the answer with the highest probability as the correct answer to question one. On 988 images the participants chose 1.1 and on 5,094 images they chose 1.2 as an answer to question 1 with more than 0.8 measure of agreement.

We trained the baseline model and CapsNet for this scheme for 200 epochs with a batch size of 20 and reported the accuracies in Table 2. The training took 1 hour and 3 hours for the baseline model and CapsNet, respectively. In terms of the number of parameters, baseline model had 209,975,554 while CapsNet had 28,276,672 for this training scheme. We show the accuracy curves versus number of

Model	Training	Testing
Baseline	100%	96.96%
CapsNet	100%	98.77%

Table 2. Training and testing accuracy vs number of epochs for classification based on the answers to question one; A relative error reduction of 59.8% was achieved.

epochs for both training and testing in Figure 3. As we can see, while the baseline model and CapsNet had similar performance during training, CapsNet outperformed the baseline model at test time. Furthermore, we show the reconstructed images at 10, 100 and 200 epochs generated by CapsNet versus the original images in Figure 4. These reconstructed images are very detailed.

In order to check whether reconstructed images preserved physical properties of the original images, we used brightness profiles of the galaxies to indicate the Sérsic index (Sérsic 1963) for each galaxy. The Sérsic profile or the Sérsic law shows how intensity I of a galaxy changes with the distance R from its center. The Sérsic profile has the following form,

$$\log(I(R)) = \log(I_0) - kR^{1/n} \quad (9)$$

where I_0 is the intensity at $R = 0$ and n is the Sérsic index that controls the curvature of the profile. We used the GALFIT software (Peng et al. 2002) to estimate the Sérsic index for a subset of reconstructed and original images (116 samples of each) and the results can be found in Figure 5. We should note that we used a Gaussian Point Spread Function (PSF) with an average FWHM of 6 pixels that was estimated using the stars present in the field. However, Willett et al. (2013) mention that each Galaxy Zoo image was re-scaled to a variable number of arcseconds per pixel during image creation, which causes slight changes in the PSF and therefore GALFIT slightly underestimates or overestimates the Sérsic index.

Furthermore, we calculated the mean (-0.41) and 95% confidence interval ($[-1.33, 0.51]$) of the difference between the Sérsic index estimated for our sample of the original and reconstructed images ($n_{Original} - n_{Reconstructed}$) and the results can be found in Figure 6. These results indicate that the reconstructed images fairly preserved the Sérsic profile of the original images. However, the estimated Sérsic index for reconstructed images are mostly larger than the original counterparts. The reason behind this is that the reconstructed images have stronger and spatially larger central light sources than original images; therefore, the estimated Sérsic indexes are larger for them.

6 CONCLUSIONS

In this work, we presented a new method for performing morphological classification of the galaxies. We used a recently introduced neural network structure called Capsule Network in two different scenarios.

In the first scenario, we trained models to predict the true crowd-sourced probabilities using both our baseline model and CapsNet. As shown in Table 1, CapsNet clearly outperforms the baseline CNN.

In the second scenario, we chose objects where the participants had more than 0.8 agreement when answering ques-

tion 1 from the question tree in the Galaxy Zoo project. Next, we chose the answer with the highest probability to be the class of the object. As we can see in Table 2, CapsNet outperformed the baseline CNN. We also reconstructed galaxy images using the decoder part of CapsNet that were very detailed and very close to their original counterparts. Furthermore, the Sérsic index of the galaxies shows that the reconstructed images preserve the physical properties of the original images. However, the estimated Sérsic index for the reconstructed images is higher than the estimated Sérsic index of their original counterparts. This can be explained by a larger central light source in the reconstructed images. Thus, training the network on larger datasets with more resolution will be a possible solution to improve this result.

CapsNet worked really well despite the fact that we did not do any data augmentation and view point extraction similar to Dieleman et al. (2015) and our network is much shallower compared to the one presented in their work. Another thing to note is that the CapsNet proposed here has many fewer parameters compared to the baseline CNN. Therefore, we believe that CapsNet is more suitable for the task of galaxy morphological classification. However, we should note that the current implementations of the routing by agreement is slow and more work is needed to reduce the computational complexity.

We should note that in our work we used the same number of capsules and the same values for λ, m^+ and m^- as in Sabour et al. (2017). In the future, we would like tune the depth of the network and the number of capsules used in the network along with the different values of the parameters. Additionally, it would be interesting to apply CapsNet on larger and more recent datasets generated by the Galaxy Zoo project. Furthermore, extending to multiple GPUs will help to overcome the limitations of our pilot study.

Upcoming large sky surveys such as LSST will increase the amount of data on galaxies dramatically and an automated method for tasks like morphological classification is highly needed. The method presented here is a possible solution for such tasks.

ACKNOWLEDGEMENTS

This work was supported in part by an allocation of computing time from the Ohio Supercomputer Center.

Funding for the SDSS and SDSS-II has been provided by the Alfred P. Sloan Foundation, the Participating Institutions, the National Science Foundation, the U.S. Department of Energy, the National Aeronautics and Space Administration, the Japanese Monbukagakusho, the Max Planck Society, and the Higher Education Funding Council for England. The SDSS website is <http://www.sdss.org/>.

The SDSS is managed by the Astrophysical Research Consortium for the Participating Institutions. The Participating Institutions are the American Museum of Natural History, Astrophysical Institute Potsdam, University of Basel, University of Cambridge, Case Western Reserve University, University of Chicago, Drexel University, Fermilab, the Institute for Advanced Study, the Japan Participation Group, Johns Hopkins University, the Joint Institute for Nuclear Astrophysics, the Kavli Institute for Particle Astrophysics and Cosmology, the Korean Scientist Group, the

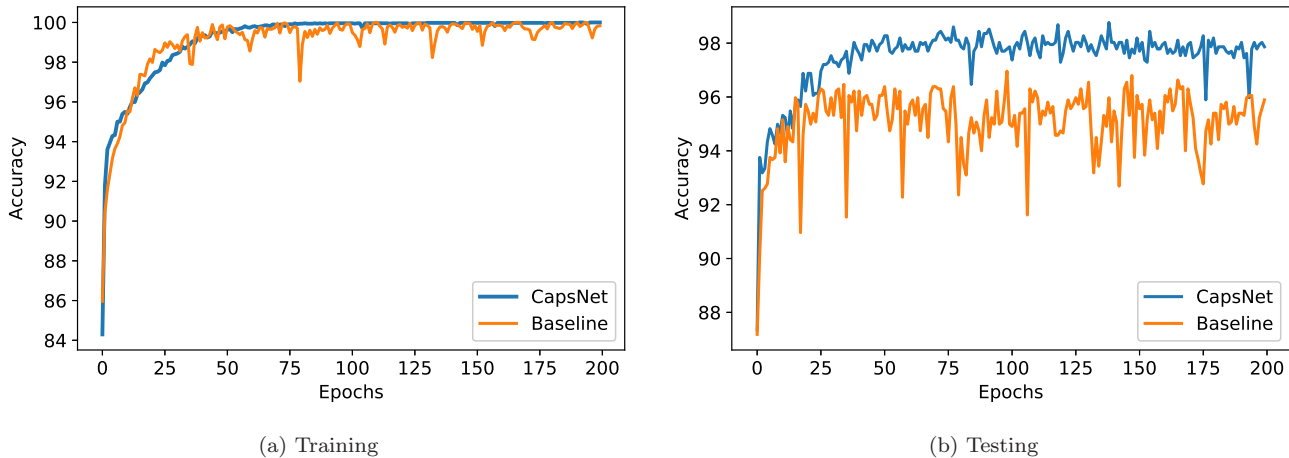


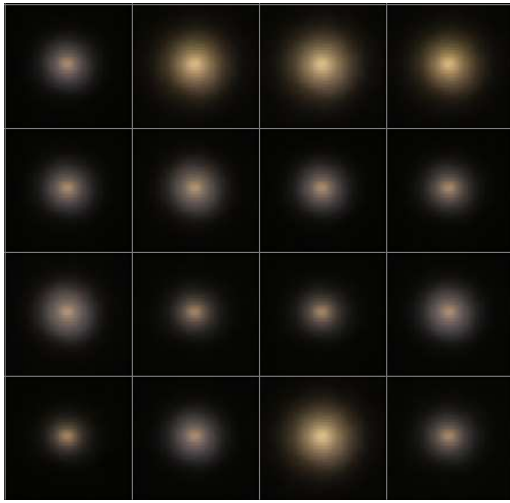
Figure 3. Training and testing accuracy vs number of epochs for classification based on the answers to question one.

Chinese Academy of Sciences (LAMOST), Los Alamos National Laboratory, the Max-Planck-Institute for Astronomy (MPIA), the Max-Planck-Institute for Astrophysics (MPA), New Mexico State University, Ohio State University, University of Pittsburgh, University of Portsmouth, Princeton University, the United States Naval Observatory, and the University of Washington.

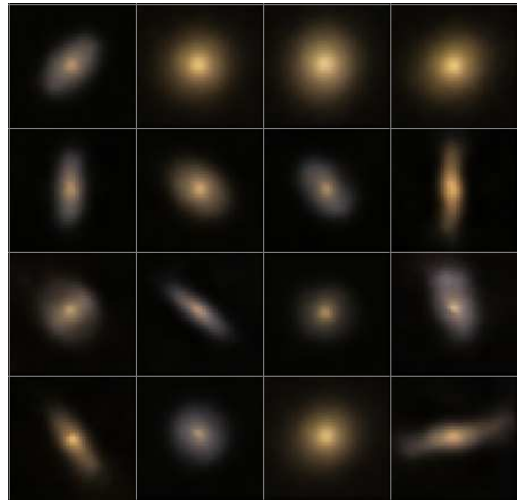
REFERENCES

- Bamford S. P., et al., 2009, *Monthly Notices of the Royal Astronomical Society*, 393, 1324
- Blanton M. R., et al., 2017, *The Astronomical Journal*, 154, 28
- Center O. S., 1987, Ohio Supercomputer Center, <http://osc.edu/ark:/19495/f5s1ph73>
- Collister A. A., Lahav O., 2004, *Publications of the Astronomical Society of the Pacific*, 116, 345
- De La Calleja J., Fuentes O., 2004, *Monthly Notices of the Royal Astronomical Society*, 349, 87
- Dieleman S., Willett K. W., Dambre J., 2015, *Monthly notices of the royal astronomical society*, 450, 1441
- Firth A. E., Lahav O., Somerville R. S., 2003, *Monthly Notices of the Royal Astronomical Society*, 339, 1195
- Glorot X., Bordes A., Bengio Y., 2011, in *Proceedings of the Fourteenth International Conference on Artificial Intelligence and Statistics*. pp 315–323
- Hinton G. E., Srivastava N., Krizhevsky A., Sutskever I., Salakhutdinov R. R., 2012, arXiv preprint arXiv:1207.0580
- Ivezic Z., et al., 2008, arXiv preprint arXiv:0805.2366
- Krizhevsky A., Sutskever I., Hinton G. E., 2012, in *Advances in neural information processing systems*. pp 1097–1105
- Kuminski E., George J., Wallin J., Shamir L., 2014, *Publications of the Astronomical Society of the Pacific*, 126, 959
- Lahav O., et al., 1995, *Science*, 267, 859
- Lintott C. J., et al., 2008, *Monthly Notices of the Royal Astronomical Society*, 389, 1179
- Naim A., Lahav O., Sodre Jr L., Storrie-Lombardi M., 1995, *Monthly Notices of the Royal Astronomical Society*, 275, 567
- Nair V., Hinton G. E., 2010, in *Proceedings of the 27th international conference on machine learning (ICML-10)*. pp 807–814
- Peng C. Y., Ho L. C., Impey C. D., Rix H.-W., 2002, *The Astronomical Journal*, 124, 266
- Sabour S., Frosst N., Hinton G. E., 2017, in *Advances in Neural Information Processing Systems*. pp 3859–3869
- Sérsic J., 1963, *Boletín de la Asociación Argentina de Astronomía La Plata Argentina*, 6, 41
- Skibba R. A., et al., 2009, *Monthly Notices of the Royal Astronomical Society*, 399, 966
- Storrie-Lombardi M., Lahav O., Sodre Jr L., Storrie-Lombardi L., 1992, *Monthly Notices of the Royal Astronomical Society*, 259, 8P
- Tasca L., et al., 2009, *Astronomy & Astrophysics*, 497, 743
- Willett K. W., et al., 2013, *Monthly Notices of the Royal Astronomical Society*, 435, 2835
- Willett K. W., et al., 2016, *Monthly Notices of the Royal Astronomical Society*, 464, 4176
- gram ai 2018, [gram-ai/capsule-networks](https://github.com/gram-ai/capsule-networks), <https://github.com/gram-ai/capsule-networks>

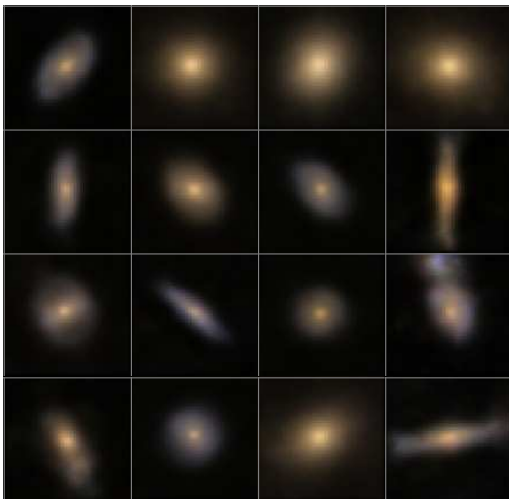
This paper has been typeset from a T_EX/L^AT_EX file prepared by the author.



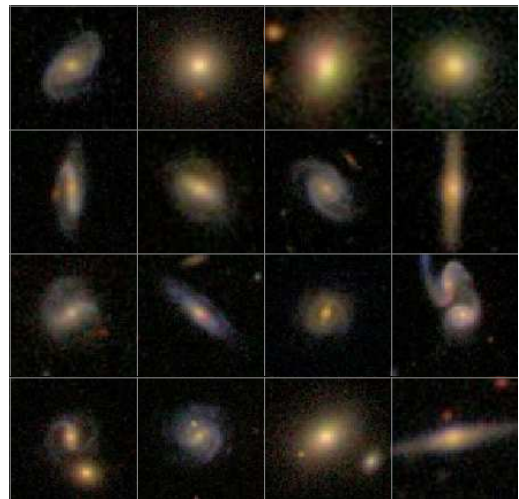
(a) Reconstruction after 10 epochs



(b) Reconstruction after 100 epochs



(c) Reconstruction after 200 epochs



(d) Original images

Figure 4. Original and reconstructed images of the galaxies.

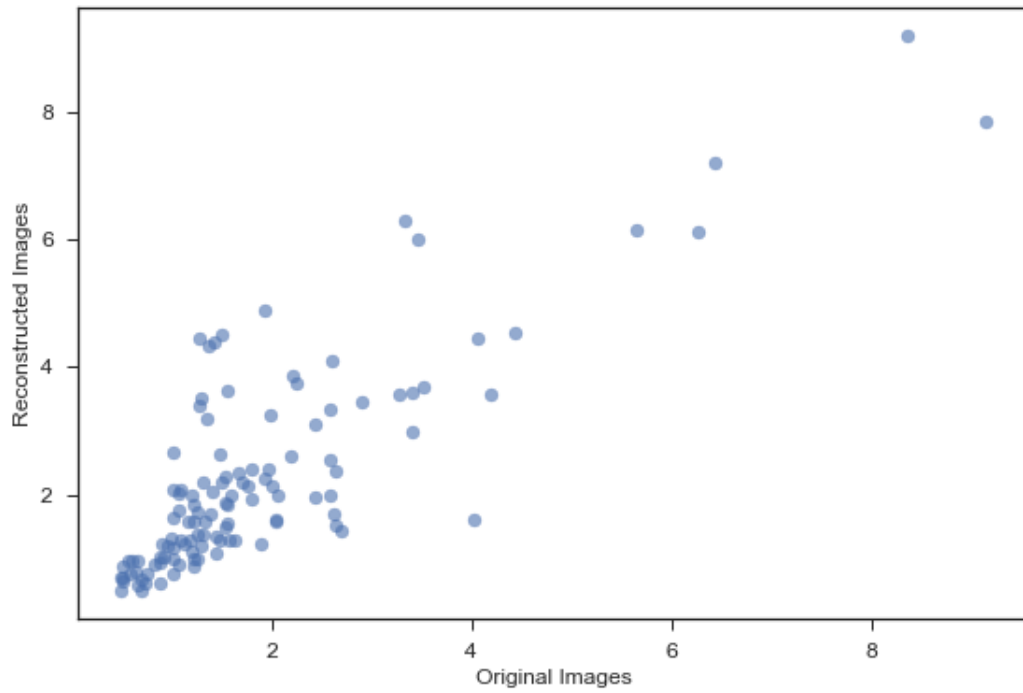


Figure 5. Estimated Sérsic index of original images versus reconstructed images.

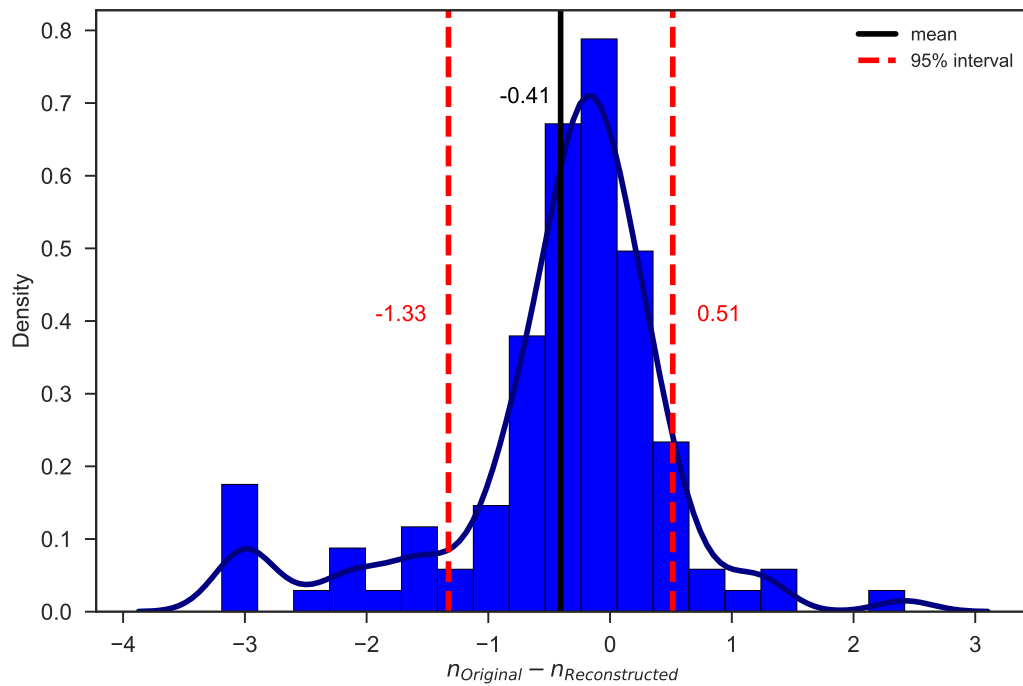


Figure 6. Mean and 95% confidence interval of the difference between the estimated Sérsic index for the original and reconstructed images ($n_{Original} - n_{Reconstructed}$).